Forecasting Research

Forecasting Research Division
Technical Report No. 195

Data Impact on UM forecasts for 12GMT 25 November 1995 (CFO workshop, January 1996)

by

R J Graham and S R Anderson

July 1996

Meteorological Office
London Road
Bracknell
Berkshire
RG12 2SZ
United Kingdom

Forecasting Research
Technical Report No. 195

Data Impact on UM forecasts for 12GMT 25 November 1995 (CFO workshop, January 1996)

by

R J Graham and S R Anderson

July 1996

Forecasting Research
Meteorological Office
London Road
Bracknell
Berkshire
RG12 2SZ
United Kingdom

© Crown Copyright 1996

This paper has not been peer-reviewed and should be regarded as an Internal Report from the Meteorological Office. Permission to quote from it should be obtained from the above Meteorological Office division.

Data Impact on UM forecasts for 12GMT 25 November 1995 (CFO workshop, January 1996)

R J Graham and S R Anderson
Observation Evaluation Group, NWP Division

1. Introduction

Forecasts from the global UM for the UK area valid 25 November 1995 gave consistently misleading guidance at ranges T + 72 and greater. The T + 60 forecast, though still with shortcomings, was a significant improvement on the T + 72 forecast. The greater skill of the T + 60 over the T + 72 implies a marked benefit from the additional data used in the later (T + 60) run. This study aims to identify the types of data which delivered the major part of this benefit. When combined with results from other case studies, results give insight into which data types most frequently contribute to cases of marked data impact.

A second aim is to identify the geographical location of the influential data. This helps to isolate regions of "sensitivity", in which small errors in initial conditions may grow rapidly in the forecast, and to relate these sensitive regions to specific meteorological features (e.g. PV anomalies).

2. Identifying the observation types that contribute the most impact

2.1 Method

To assess the impact of various observation types we perform a series of model runs each comprising a 60hr forecast verifying at 12GMT 25 November, preceded by a 12hr analysis cycle (12GMT 22 Nov to 00GMT 23 Nov) during which the observations to be assessed are assimilated. Two control runs are performed. One uses all the available data (the AllOBS run); the other entails a dummy assimilation using no data (the NoOBS run). The NoOBS run is equivalent to the "poor" T + 72 operational forecast, while the AllOBS is equivalent to the "better" T + 60 operational forecast. The benefit of the data assimilated is measured according to the reduction in rms PMSL forecast error, achieved relative to the AllOBS control, over the area of interest.

2.2 The NoOBS and AllOBS control forecasts

Figs.1a-c show, respectively, the verifying PMSL analysis valid 12GMT 25 November, and the NoOBS and AllOBS forecasts. The verifying analysis (Fig.1a and reference to previous charts, not shown) shows that strong development to the west of Scotland has formed a low pressure centre (***A***, ~992hPa) at the western

end of an elongated depression extending to the coast of Norway. Another low centre (***B***) is located over Cornwall with an associated trough extending to Iberia.

In the NoOBS run (Fig.1b) there is no development to the west of Scotland. The elongated depression has progressed eastward to the coast of Norway leaving only a weak trough extending westwards towards the true location of ***A***. A ridge has developed over Scotland, south-west of the low. The eastward movement of low ***A*** has led to disruption from low ***B*** which is erroneously represented as a detached feature located west of Iberia.

The AllOBS run (Fig.1c) clearly still has shortcomings. However, there are some significant improvements on the NoOBS run. Notably there has been much greater cyclonic development over and west of Scotland, and consequently less eastward progression of low ***A***. The difference between the AllOBS and NoOBS PMSL forecasts are plotted in Fig.1d and show PMSL values to be some 16hPa lower in the AllOBS run near the observed position of low ***A***, demonstrating a clear positive data impact (recall that the differences represent the impact of all observations used in the operational analysis cycle 12GMT 22 to 00GMT 23 November).

The AllOBS forecast for low ***B*** is also superior to the NoOBS forecast. In particular, the low centre is located further north-east, and has less of the characteristic "cut off" appearance evident in the NoOBS run (Fig.1b).

2.3 Identification of the key observation types

In this section we identify the observation types that made the key contributions to the "AllOBS" impact described in section 2.2. This is achieved by evaluating the benefit delivered by each observation type when used alone in the assimilation. Results are shown in Table 1, in which observation benefit to forecasts of PMSL is expressed as a percentage of the benefit obtained with all observations (the AllOBS benefit). Radiosonde temperatures and conventional surface data (P* and, over oceans, wind) make the most substantial impacts at 51% and 28% of the AllOBS impact, respectively. A run using both radiosonde temperatures and surface data (RsTSFC) gave 109% of the AllOBS benefit (i.e. a better forecast than obtained when all the available data is used). Use of radiosonde temperatures and conventional surface data alone is therefore sufficient to reproduce the benefit obtained from all the available data. The fact that the RsTSFC run is slightly better than the AllOBS run suggests that one or more of the data types used in the AllOBS run had a negative impact on the forecast.

The impact from radiosonde temperatures may be seen in Figs.2a&b which show, respectively, results from the run using only radiosonde temperatures (the RsT run) and the (RsT-NoOBS) difference. On first inspection the RsT impact seems disappointing, since there is little change in the shape of the flow pattern relative to that of the NoOBS forecast (ref Fig.1b). However, reference to the differences (Fig.2b) shows that positive impacts are evident, in the form of a westward shift of the low near Norway and a northward shift of low ***B***.

Results from the run in which both radiosonde temperatures and

conventional surface data are presented to the assimilation (RsTSFC) are shown in Figs.3a. It is clear that use of the surface data adds a great deal to the benefit. Most notably a marked trough is present to the west of Scotland close to the true position of low ***A***. In addition the ridge over Scotland (an erroneous feature in both the NoOBS and RsT runs) has been eroded. Fig.3b shows the difference between the RsTSFC and RsT runs, and clearly shows the main impact of the surface data to be further reduction in PMSL (around 12.5hPa) in the vicinity of low ***A***.

RUN NAME	OBSERVATION TYPE USED	% OF ALL OBS BENEFIT
AllOBS	ALL OBS	100
RsT	RADIOSONDE TEMPERATURES	51
SFC	SURFACE DATA (conventional pressure and, over oceans, wind)	28
RsH	RADIOSONDE HUMIDITIES	13
RsW	RADIOSONDE WINDS	10
SCT	SCATTEROMETER 10M WINDS	6
AcW	AIRCRAFT WINDS	3
NoOBS	NO OBS	-
CTW	CLOUD TRACK WINDS	0
SaT	SATELLITE TEMPERATURES	-3
AcT	AIRCRAFT TEMPERATURES	-7
RsTSFC	RADIOSONDE TEMPERATURES + SURFACE DATA	109

Table 1: Benefit obtained with single (and combinations of) observation types. Benefit is calculated using rms error in PMSL, using the formula,

$$\%\ \text{OF ALL OBS BENEFIT} = \frac{[\text{RMSE(NO OBS)} - \text{RMSE(OB TYPE)}]}{[\text{RMSE(NO OBS)} - \text{RMSE(ALL OBS)}]} \times 100$$

over the area 25-05W,50-65N.

3. Finding the location of the important radiosonde and surface observations

To find the location of the important radiosonde and surface data a number of model runs were performed in which only observations from specific geographical areas, thought to contain important features of the flow, were assimilated. A first estimate of the location of these "sensitive" areas is obtained by tracing differences in the NoOBS and AllOBS forecasts for low ***A*** back to the analysis time. Potential vorticity (PV) on the 300K surface and potential temperature (θ) on the 850hPa surface have been found to be useful diagnostics for this purpose, because of their conservative properties and their relationship with surface development (Hoskins et.al.,1985). The main results from these experiments is given in section 3.1 and 3.2, a detailed account is given in Appendix A.

3.1 Location of the radiosonde data important for this case

Reference to the evolution of upper-level PV and low-level θ fields (see Appendix A) suggested two areas where use of radiosonde temperature profiles at analysis time may have played an important role in improving the forecast. These two areas are shown in Fig.4. The first area (full line in Fig.4) comprises NE Canada and western Greenland (45-90N 90-45W) and will be referred to as the "upstream" area; the second area (dashed line) comprises Iceland and the bulk of Greenland (60-90N, 60-05W), and will be referred to as the "downstream" area. Land stations (R) and ships (U) from which at least one radiosonde ascent was assimilated in the 12hr cycle, 12GMT 22 to 00GMT 23 November are also shown in Fig.4. A sparse coverage of radiosonde information may be seen in both upstream and downstream areas.

Table 2 shows an evaluation of forecasts obtained when radiosonde temperature observations in these two areas are the only data presented to the assimilation. Use of radiosonde temperature data from the upstream area (run RsTU) is evidently more beneficial than use of radiosonde temperature data from the downstream area (run RsTD), in this case; data in the upstream area achieves 41% of the AllOBS benefit, while data in the downstream area achieves 24%. Use of radiosonde temperatures over the union of the two areas (run RsTUD) delivers the same benefit as global use (51%, cf. Table 1), this implies that the downstream and upstream areas contain all the radiosonde data important to obtain the forecast benefit, for this case, over the UK region.

Further experimentation found that, when combined with surface data, radiosonde data analysed on model levels 4-9 delivers the major part of the benefit (model levels 4-9 represents, approximately, the pressure interval 850hPa to 400hPa, except near high orography). The experiments performed are described in more detail in Appendix B.

An important point, discussed in more detail in Appendix A, is that the potential vorticity anomaly directly associated with the development of low ***A*** was located in the downstream area at analysis time. The important contribution from

the upstream area is therefore transmitted indirectly by the process of downstream development.

RUN NAME	EXPERIMENT DESCRIPTION	% OF ALL OBS BENEFIT
RsTD	Radiosonde temperatures downstream area	24
RsTU	Radiosonde temperatures upstream area	41
RsTUD	Radiosonde temperatures downstream area and upstream area	51

Table 2: Benefit obtained when radiosonde temperature information from specific areas is the only data presented to the assimilation
Benefit is calculated according to;

$$\%\ \text{OF ALL OBS BENEFIT} = \frac{[\text{RMSE(NO OBS)} - \text{RMSE(OB TYPE)}]}{[\text{RMSE(NO OBS)} - \text{RMSE(ALL OBS)}]} \times 100$$

over the area 25-05W,50-65N.

3.2 Location of surface data important for this case

Examination of the PV and θ evolution suggested two areas where use of surface data in the initial analysis may have had an impact on the forecast. The areas are shown in Fig.5. The first area (45-90N 90-40W, full line) is similar to the upstream area of section 3.1, but extends 5deg further east. The second area (dashed line) includes Iceland and the eastern-central Atlantic (40-10W 40-70N), and will be referred to as the "Atlantic" area. The surface information used in the 12hr assimilation cycle is also shown in Fig.5. Coverage in the upstream area decreases with increasing latitude, and north of 60N consists largely of coastal stations on Greenland and Baffin Island. The Atlantic area has reasonable coverage from ships and from drifting buoys, and dense coverage from SYNOPS over Iceland.

Table 3 shows an evaluation of forecasts obtained when surface data from the upstream and Atlantic areas shown in Fig.5 are added to radiosonde temperature data from the upstream and downstream areas shown in Fig.4 (i.e. run RsTUD). Use of surface data from the upstream area (run RSFCU) clearly adds more to the radiosonde benefit than surface data from the downstream area (run RSFCA), the former giving 85% of the AllOBS benefit, the latter 61%. Use of surface information from both Atlantic and upstream areas gives 91% of the AllOBS benefit and indicates that most of the influential surface data is within the union of the upstream and "Atlantic"areas.

RUN NAME	EXPERIMENT DESCRIPTION	% OF ALL OBS BENEFIT
RSFCA	RsTUD + Surface observations Atlantic area	61
RSFCU	RsTUD + Surface observations upstream area	85
RSFCAU	RsTUD + Surface observations from both upstream and Atlantic areas	91

Table 3: As table 2 but showing the additional impact delivered by surface information adds to the impact of the RsTUD run.

4. Further studies

During the course of investigation a number of supplementary results were obtained. These results are discussed briefly below.

4.1 Large O-B differences in the PMSL observation from Eureka, Canada

Observation minus background (O-B) information from the operational Observation Processing Database (OPD) shows that the PMSL observations from station 71917 at Eureka, Ellesmere Island, Canada (located in the "upstream"area, and ringed in Fig.5) were typically 5hPa higher than collocated model values during the assimilation period. This high bias is reflected in the (O-B) statistics for November 1995 which show a mean value of +3.2hPa (and a standard deviation of 1.8hPa). Monitoring statistics from ECMWF show a significantly smaller bias of +0.6hPa (standard deviation, 1.6hPa) (personal communication, Bernard Strauss). The more acceptable bias value for the ECMWF model suggests either that the UM has a low pressure bias in this region, or that there is a problem in interpolating the PMSL observation onto pressure at the model surface. The first possibility seems unlikely since observations from neighbouring stations do not show a marked PMSL bias with UM values.

4.2 The impact of NESDIS TOVS data

One possible reason for differences between the UKMO and ECMWF model forecasts is the different use of data in the assimilation schemes used at each centre. One major difference is in the use of TOVS temperature soundings. At ECMWF direct use is made of the TOVS radiance information, using a 1-D VAR pre-processing scheme. In contrast the UKMO, at the time of this case, were

assimilating NESDIS retrievals of layer mean temperature. (Direct use of radiance information has since been implemented in the operational model, using the GLOSS processing scheme (Gadd et al., 1995)). It has been shown (Gadd et al., 1995; Eyre et.al, 1993) that direct use of TOVS radiances increases the positive impact of the TOVS information on NWP forecasts.

The importance of temperature profiles in this case, proved by the marked impact from radiosonde temperature profiles (Table 2), suggests that the better use made of TOVS data in the ECMWF system might be a reason for the better forecasts from the ECMWF model. This possibility is supported by the fact that the NESDIS retrieved layer temperatures have a negative impact on the UKMO forecasts. This has been demonstrated by adding NESDIS TOVS to the RsTSFC run (radiosonde temperatures and surface data only). Addition of NESDIS TOVS decreases the benefit from 109% of AllOBS (Table 1) to 84%. Fig.6 shows the differences between the RsTSFC run and the run with NESDIS TOVS added (the RsTSFC PMSL forecast is shown in Fig.3a). It may be seen that inclusion of NESDIS TOVS reduces the cyclonic development to the west of Scotland by around 4hPa.

The above result suggests that use of GLOSS processing of TOVS information may significantly improve the UM forecast in this case. We recommend that an experiment to test this hypothesis be conducted.

5. Conclusions

The main conclusions of the study are summarised below.

- Radiosonde temperature profiles and conventional surface data (P* and, over oceans, wind) contributed the main part of the observed data benefit to forecasts for the UK region. The most influential observations were located over NE Canada and western Greenland, with impact on the forecast being transmitted indirectly by a process of downstream development.

- Most of the impact from radiosonde temperatures came from data analysed on model levels 4 to 9 (representing approximately, and away from high orography, the 850hPa to 400hPa layer) .

- Use of surface data was essential to obtain the cyclonic development to the west of Scotland in the 60hr forecast.

- Use of NESDIS TOVS retrievals significantly degraded the forecast.

Points of general interest, highlighted by this case are listed here.

- Radiosonde temperatures are usually reported with a collocated wind observation. However, sole use of radiosonde winds did not achieve the substantial impact obtained with sole use of radiosonde temperatures (10% for winds compared to 51% for temperatures, Table 1). This implies that the strategy of assimilating temperature increments derived from analysed wind increments (a sub-procedure of the assimilation scheme), was unable (in this case) to reproduce the crucial information contained in the radiosonde temperature data. The general inference is that both temperature and wind profiles are beneficial to NWP forecast accuracy. However, results derived from a number of case studies (Graham and Anderson, 1995) suggest that wind profiles are useful more frequently than are temperature profiles. The importance of temperature information up to at least 400hPa in this case suggests that Radio Acoustic Sounding Systems (RASS) may frequently fail to sample temperature structures important for short to medium range forecasts. A 404Mhz system, for example, has a max vertical range of about 4.5km (~650hPa). A 50MHz system has a higher range, but has a lowest measurement gate of ~2km) (Martner et.al., 1993).

- The important role of temperature profiles in this case suggests that high resolution temperature sounders (planned to fly on the ESA METOP polar orbiting satellite series, launch ~2002) will bring valuable impacts. These instruments will give global coverage of temperature profiles with a vertical resolution commensurate with that of global NWP models.

- The important role of surface data supports evidence (Graham and Anderson, 1995) that the surface observation network is valuable to global-scale NWP.

6. Recommendations

- We recommend that a further experiment be conducted to assess the benefit of assimilating GLOSS processed TOVS data in place of NESDIS retrievals.

- The reason for the large positive (O-B) bias in PMSL reports from Eureka (71917) during November 1995 should be investigated (no similar bias is observed in (O-B) statistics from ECMWF).

References

Cullen, M J P 1993: *The Unified Forecast/Climate Model*, Meteorol. Mag.,122, No.1449, 81-93

Eyre,J.R.,Kelly,G.A. McNally,A.P., Anderson,E. and Persson,A 1993: *Assimilation of TOVS radiance information through one-dimensional variational analysis* Quart.J.Roy.Meteor.Soc.,119,1427-1463.

Gadd,A.J., Barwell,B.R., Cox,S.J and Renshaw,T.J. 1995: *Global processing of satellite sounding radiances in a numerical weather predict system*. Quart.J.Roy.Meteor.Soc.,119, 615-630.

Martner,B.E., Wuertz,D.B., Stankov,B.B., Strauch,R.G. Westwater,E.R. Gage,K.S. Ecklund,W.L. Martin,C.L. and Dabberdt,W.F. 1993: *An evaluation of Wind Profiler, RASS and Microwave Radiometerperformance*. Bull. Amer. Met. Soc.,74,4,599-613

Graham, R J and Anderson, S 1995: *The relative utility of current observation systems to global-scale NWP forecasts; preliminary results*. UK Met. Office FR Division Tech. Report No.173

Hoskins, B J, McIntyre, M E and Robertson, A W 1985: *On the use and significance of isentropic potential vorticity maps*. Quart.J.Roy.Met.Soc., 111, 877-946.

APPENDIX A

Data impact on forecasts for 12GMT 25 November 1995: a PV perspective

Throughout this appendix use is made of the "PV thinking" ideas described by Hoskins et.al (1985).

1. The relationship between low A and the PV and θ distribution

Fig.A1a shows the PV analysis on the 300K surface and θ analysis on the 850hPa surface, valid at 12GMT 25 November, the location of low ***A*** is also shown ("•"). Low ***A*** is associated with an upper-level PV anomaly (***D***) centred south-west of Ireland. The anomaly is "cut-off" from the polar "reservoir" of high PV air and has consequently become slow moving. Another, weaker, anomaly (***E***) is centred south of Iceland. A tongue of low-level warm air (***T***) has become drawn around the northern flank of anomaly ***D*** in a typical upper-level/lower-level "phase-locking" development. Low ***A*** is located within this warm tongue.

Comparison of the PV distribution in the NoOBS forecast (Fig.A1b) with Fig.A1a suggests that the flow pattern was too mobile in the NoOBS run. Anomaly ***D*** is located north-east of its true position and is not a cut-off feature but is merged with anomaly ***E***, the latter being some 15deg east of its true position. The surface warm tongue (***T***) has been carried east of its correct position through phase-locking with anomaly ***D***. The failure to forecast ***D*** as a cut-off anomaly has resulted in insufficient westward extension of the warm tongue. Consequently little cyclonic development was forecast to the west of Scotland (compare Figs.1a and 1b, main report).

The PV and θ forecast from the AllOBS run (Fig.A1c), although deficient in a number of ways, shows some important improvements over the NoOBS run. North of 60N the AllOBS run is clearly superior, with less eastward progression of the high PV air. Near 60N the AllOBS run has produced a single PV anomaly located mid-way between the true positions of anomalies ***E*** and ***D***. This anomaly has induced a weak warm ridge in the isotherms in a similar location to the warm tongue (***T***) seen in the analysis (Fig.A1a). The warm ridge is located over the true position of low ***A***, and is associated with the trough seen in that position in the AllOBS PMSL forecast (Fig.1c, main report).

Fig.A1d shows the difference between the AllOBS and NoOBS PV and θ fields. The PV differences show a dipole structure with the positive pole located near 15W, west of the negative pole (reflecting the more westward position of the high PV air in the AllOBS run). A positive difference in the θ field is evident below the positive pole of the PV difference, and reflects the greater development of the low-level "warm tongue" in the AllOBS run.

2. The impact of radiosonde temperatures on the PV and θ evolution

Figs A2a&b show, respectively, the PV and θ fields at T+0 in the NoOBS run and the AllOBS - NoOBS differences (since all difference fields in this section are with respect to the NoOBS run, reference to NoOBS will be dropped when referring to difference charts). Referring first to Fig.A2a, the high PV air from which anomalies ***D*** and ***E*** evolve may be seen over eastern Greenland and surrounding areas (labelled ***G***). The next major upstream anomaly (labelled ***H***) is located over the Hudson Bay area. The analysis differences (Fig.A2b) represent data impact on the AllOBS analysis.

The largest PV differences between the AllOBS and NoOBS runs (Fig.A2b) are associated with PV anomalies ***G*** and ***H***. Marked differences in low-level temperature may also be seen near Newfoundland, south-western and eastern Greenland and in a region centred near Iceland. The following experiments attempt to assess the importance of these differences by performing runs in which only data in the location of the differences are presented to the assimilation. Only radiosonde temperatures and surface data are used in these runs - since we have already established that use of these two data types alone is sufficient to recover the benefit obtained with all available observations (main report, Table 1).

Although we concentrate here on the evolution of the largest differences, it should be borne in mind that very small initial differences (i.e. too small to be visible in Fig.A2b) may sometimes grow rapidly and dominate the forecast differences.

Run RsTD: Impact of radiosonde temperatures sampling the "downstream" differences

In this run only radiosonde temperatures over a region referred to as the "downstream" region (60-90N,60-5W) were presented to the assimilation. The downstream region encompasses PV anomaly ***G*** and the Greenland/Iceland temperature differences. The RsTD differences at T+0 are shown in Fig.A2c. Within the area for which data were used (indicated on Fig.A2c, and also main report Fig.4) the RsTD difference field resembles the AllOBS difference field (Fig.A2b) - though the amplitude of the differences is somewhat smaller. This suggests that the assimilation of radiosonde temperatures played a significant role in producing the initial AllOBS differences associated with the downstream anomaly.

Run RsTU: Impact of radiosonde temperatures sampling the "upstream" differences

In this run only radiosonde temperatures over a region referred to as the "upstream" region (45-90N, 90-45W) were presented to the assimilation. The "upstream" region encompasses PV anomaly ***H*** and the temperature differences over Newfoundland and south-west Greenland. The RsTU differences at T+0 are shown in Fig.A2d. As for the RsTD run the differences are similar to the AllOBS differences in the area where data were used, though the amplitude is weaker.

Figs.A3a-d correspond with Figs.A2a-d, but show fields and differences at T+24. The RsTD differences associated with anomaly ***G*** (Fig.A3c) are similar in phase to the AllOBS differences (Fig.A3b), but are weaker in amplitude. In the RsTU run (Fig.A3d), differences associated with anomaly ***H*** resemble those of the AllOBS run, as at T+0. In addition, however, small differences have propagated downstream to improve the representation of anomaly ***G***. This may be appreciated by noting the positive difference south of Iceland in Fig.A3d, which is located near the positive pole of the AllOBS differences in this region. Very little of the AllOBS θ differences have been reproduced by either the RsTD or RsTU runs.

Figs.A4a-d correspond with Figs.A2a-d, but show fields and differences at T+60. Both the RsTD and RsTU differences associated with anomaly ***G*** (Fig.A4c&d) have similar phase to the AllOBS differences (Fig.4Ab), implying the desired delay in its eastward movement (the smaller scale anomalies ***D*** and ***E*** described in section 1, may be seen within anomaly ***G*** - Fig.4Aa). In contrast to the situation at T+24 (Figs.A3c&d), the amplitude of the RsTU differences is now greater than that of the RsTD differences, having undergone rapid growth. In addition, the RsTU run also exhibits positive θ differences near low ***A*** , although the amplitude is not as large as in the AllOBS differences. This low-level structure is less well reproduced by the RsTD run.

In conclusion radiosonde temperatures from both upstream areas (NE Canada and western Greenland) and downstream areas (much of Greenland) contributed to the beneficial impact. Impacts contributed by the upstream area, which appear to engage with the downstream anomaly by T+24 are the more important of the two at T+60. This is confirmed by verification of the PMSL fields from both the RsTD and RsTU runs (main report, Table 2);

3. The additional benefit obtained when surface data are added to the radiosonde temperature data

In the following experiments the radiosonde temperature information from both the upstream and downstream areas, discussed in section 2, were retained in the assimilation and conventional surface information, from two specific areas described below, were added.

Run RSFCA: Addition of surface data from eastern North Atlantic

In this run surface information from a region in the eastern North Atlantic (40-70N, 40-10W, see Fig.A5c and main report Fig.5)) were added to the radiosonde temperatures.

Run RSFCU: Addition of surface data from NE Canada and western Greenland

In this run surface information from the upstream area 45-90N, 90-40W (i.e. as the RsTU area, but extending 5deg further west - see Fig.A5d and main report Fig.5) were added to the radiosonde temperatures.

The RSFCA and RSFCU differences at T+24 are shown in Figs.A5c&d, respectively (the corresponding NoOBS field and AllOBS differences are repeated in Figs.A5a&b for ease of reference). The PV differences in both the RSFCA and RSFCU runs show close resemblance to the AllOBS differences associated with anomaly ***G***. Both runs have correctly produced a positive θ difference near 60N 15W, which is absent, or very weak, in the radiosonde temperature only runs at T+24 (RsTD, Figs.A3c and RsTU Fig.A3d). A notable difference between the runs is that the RSFCU run has generated a negative θ difference west of Iceland in the Denmark Strait, this corresponds with the AllOBS difference field, but is not seen in the RSFCA differences (which shows a small positive difference in the same area). The negative difference implies that in the RSFCU (and AllOBS) run, air moving south on the western flank of ***G*** is colder than in the NoOBS run. PV "thinking" suggests that this colder airflow will tend to contribute to a greater southward extension of anomaly ***G***, and a slowing of its eastward progression relative to the NoOBS run, which are both features of the "better" AllOBS forecast. This suggests that the significant forecast benefits delivered by surface data (main report, Fig.3b) derives, at least in part, from its role in initiating this colder air flow.

Figs.A6a-d correspond with Figs.A5a-d, but show fields and differences at T+60. The RSFCU differences (Fig.6Ad) now resemble the AllOBS differences more closely than do the RSFCA differences (Fig.6Ac). The positive pole of the PV dipole is located further west (note the proximity of the western edge to the coast of Iceland). The representation of the positive θ difference is clearly much better in the RSFCU run. The positive difference is paired with a negative difference to its west which is embedded in the aforementioned colder flow in the RSFCU run south of Greenland.

The results of the RSFCA and RSFCU runs suggest that surface information from the upstream area was more important than that over the Atlantic, though the latter also made a significant contribution. This was confirmed by verification of the PMSL forecast from both runs (see main report Table 3).

APPENDIX B

The impact of radiosonde temperatures at different levels

Three variations of the RSFCU run (see main report Table 3, and Appendix A) were performed to assess the impact of radiosonde temperatures at different model levels. Runs RSFCU1-6 used only low-level temperature data (see Table B1), run RSFCU7-19 used only upper-level data and run RSFCU4-9 used only mid-level data. Loss of impact in RSFCU1-6 and RSFCU7-19 is dramatic, from 85% of the AllOBS benefit (obtained with the full RSFCU run) to around 50%. Use of mid-level data RSFCU4-9 gives a better result at 75%. This shows that temperature profile information most important for improving the forecast was, in this case, in the layer 850hPa and 400hPa.

It is possible (but has not been proved here) that temperature profiles in mid-levels were important in this case because they provide vertical sampling of the tropopause region. This issue is relevant when considering the relative utility of aircraft and radiosonde observations of both temperature and wind. An important feature of PV anomalies is that they represent a region in which the tropopause has descended - bringing high PV stratospheric air to relatively low altitudes. In such regions aircraft operating at cruise levels (e.g. 300hPa) will often be well above the tropopause and unable to sample the associated vertical temperature gradient. For this reason it is likely that, near significant PV anomalies, radiosonde profiles may be more effective for analysis of the degree of tropopause descent (often crucial for good forecasts of the intensity of cyclogenesis) than observations from aircraft at cruise levels.

RUN NAME	EXPERIMENT DESCRIPTION	% OF ALL OBS BENEFIT
RSFCU1-6	A RSFCU (main report, Table 3), but only radiosonde data on model levels 1-6 used	52
RSFCU7-19	As above, except that only radiosonde data on model levels 7-19 used	51
RSFCU4-9	As above , except that only radiosonde data on model levels 4-9 used	75

Table B1: Experiments in which assimilation of radiosonde temperature observations was restricted to specific band of model levels.

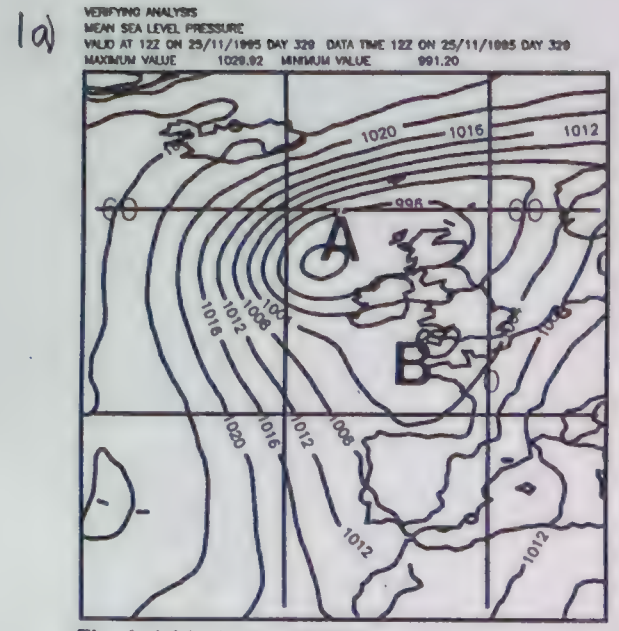

Fig.1a) Verifying PMSL analysis for 12GMT 25/11/95.

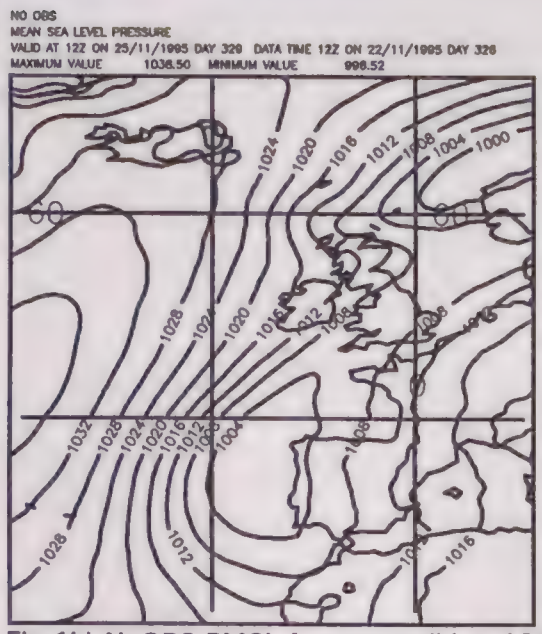

Fig.1b) NoOBS PMSL forecast valid at 12GMT 25/11/95.

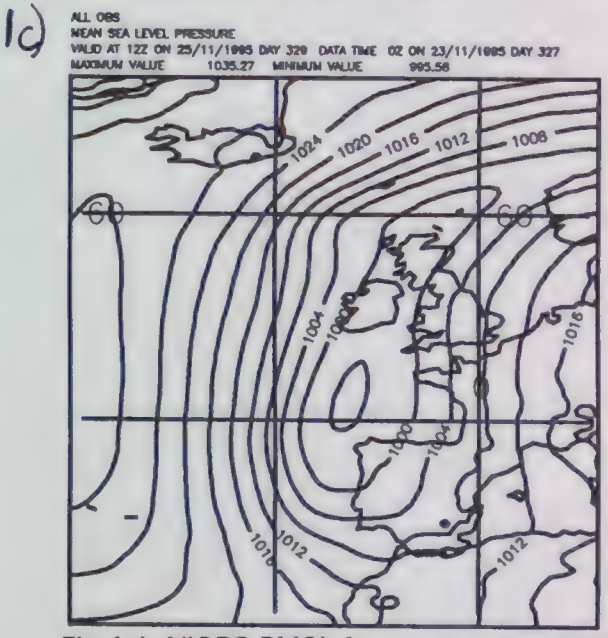

Fig.1c) AllOBS PMSL forecast valid at 12GMT 25/11/95.

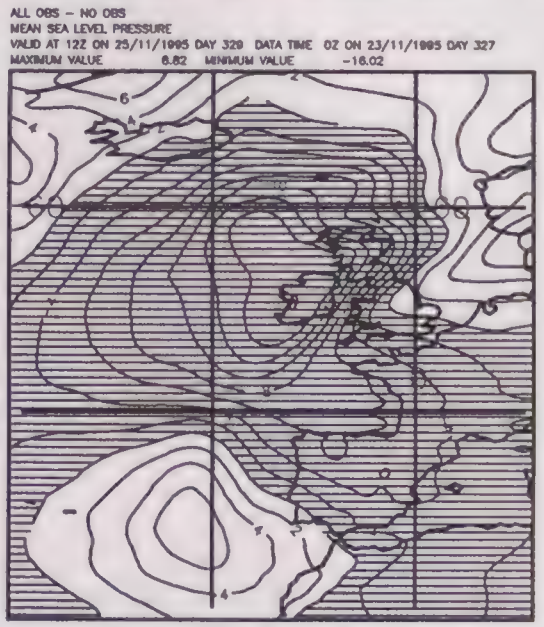

Fig.1d) Difference between AllOBS and NoOBS forecasts (AllOBS - NoOBS) valid 12GMT 25/11/95. Contour interval = 2hPa, hatching indicates negative differences.

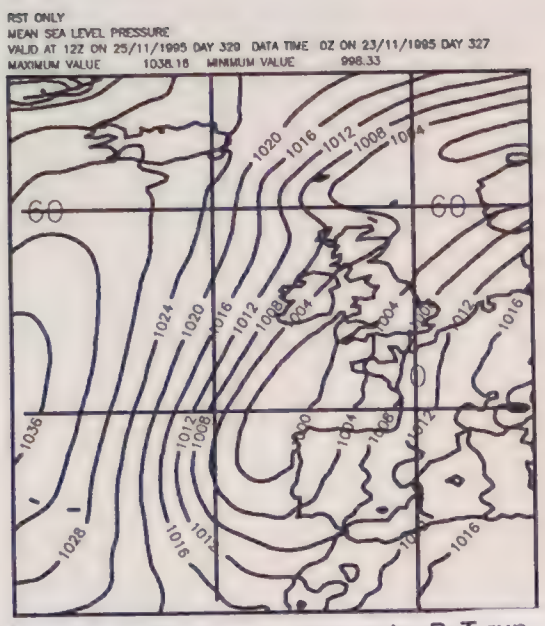

Fig.2a) PMSL forecast from the RsT run.

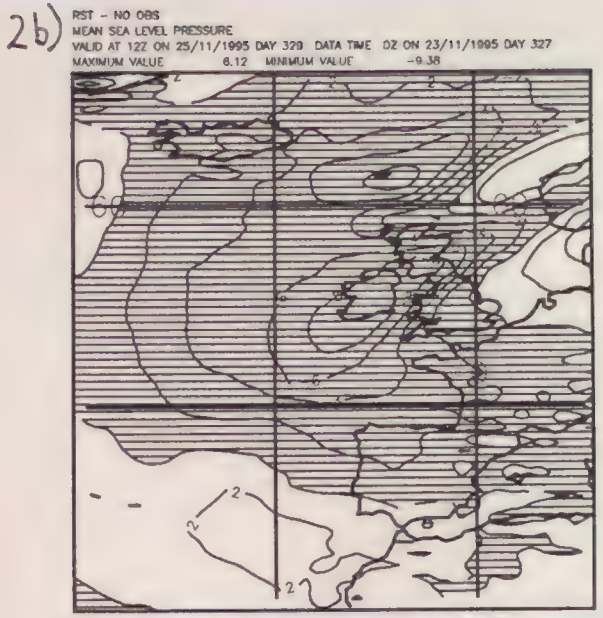

Fig.2b) As Fig.1d, but for the RsT - NoOBS difference.

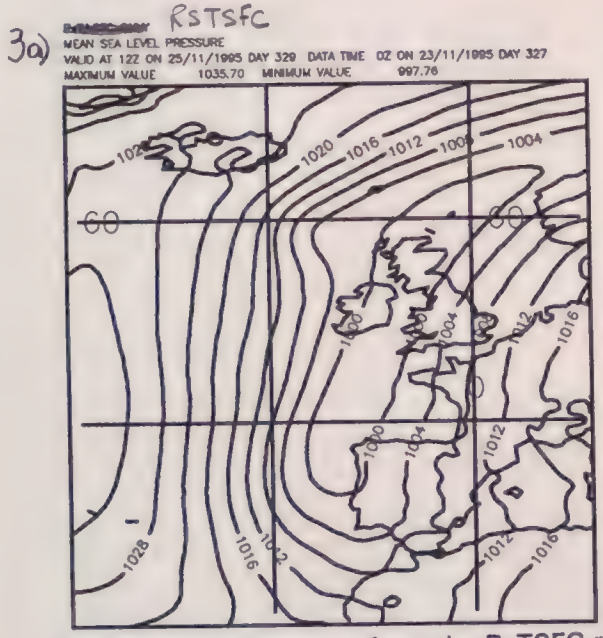

Fig.3a) PMSL forecast from the RsTSFC run.

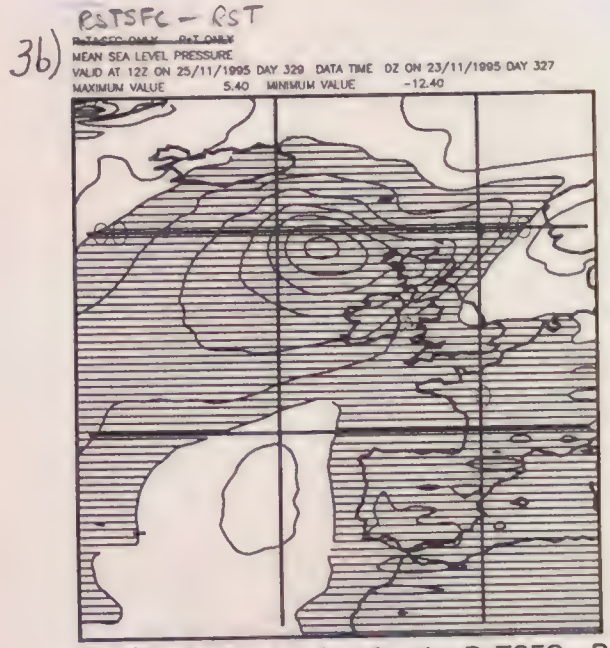

Fig.3b) As Fig.1d, but for the RsTSFC - RsT difference

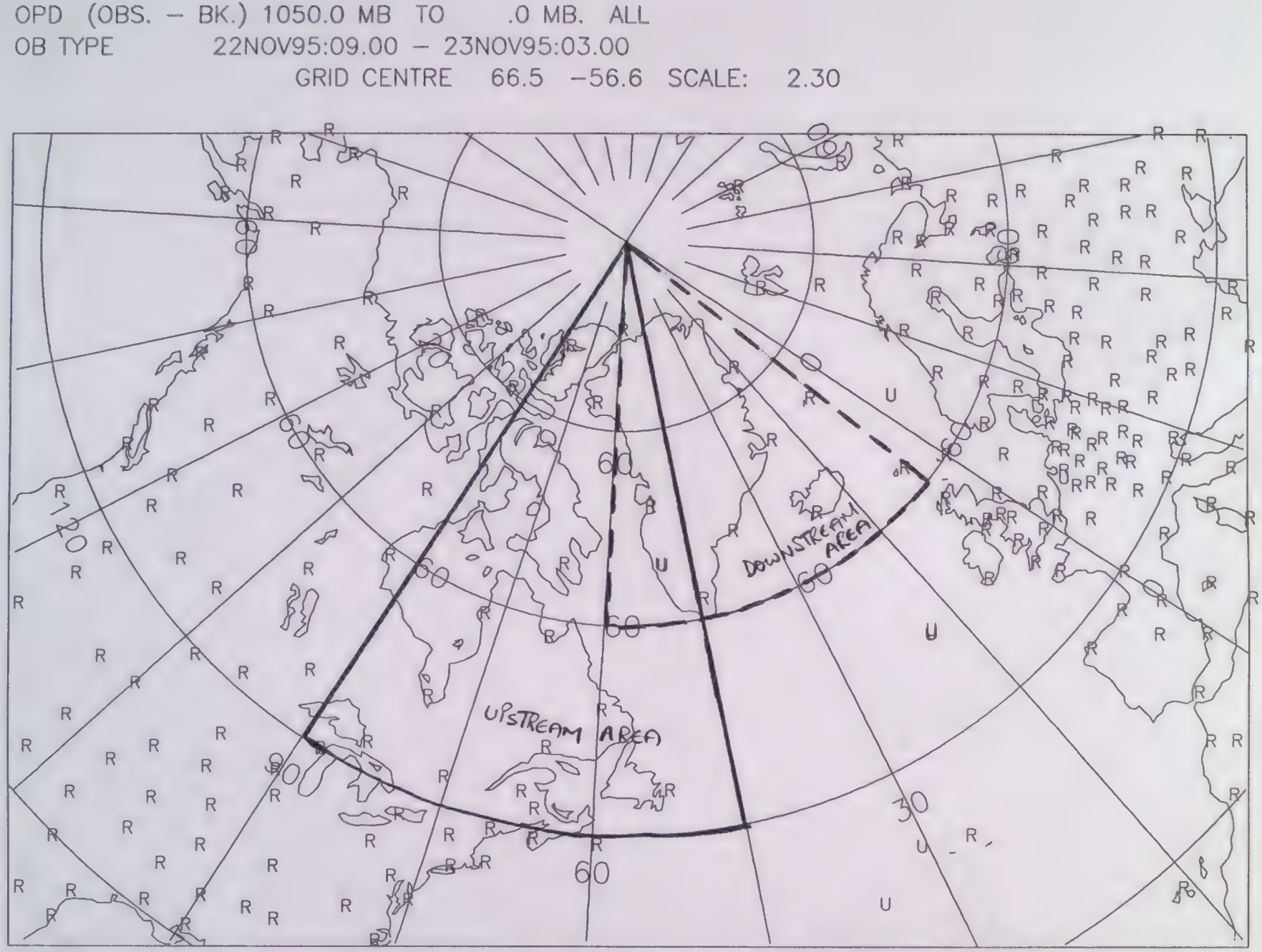

Fig.4) **The "upstream" area (full line) and "downstream" area (dashed line) defined for experiments with radiosonde temperature data.**

OPD (OBS. – BK.) SURFACE ALL

OB TYPE 22NOV95:09.00 – 23NOV95:03.00

Fig.5) The "upstream" area (full line) and "downstream" area (dashed line) defined for experiments with conventional surface data. The station at Eureka (71917), referred to in Section 4, has been ringed.

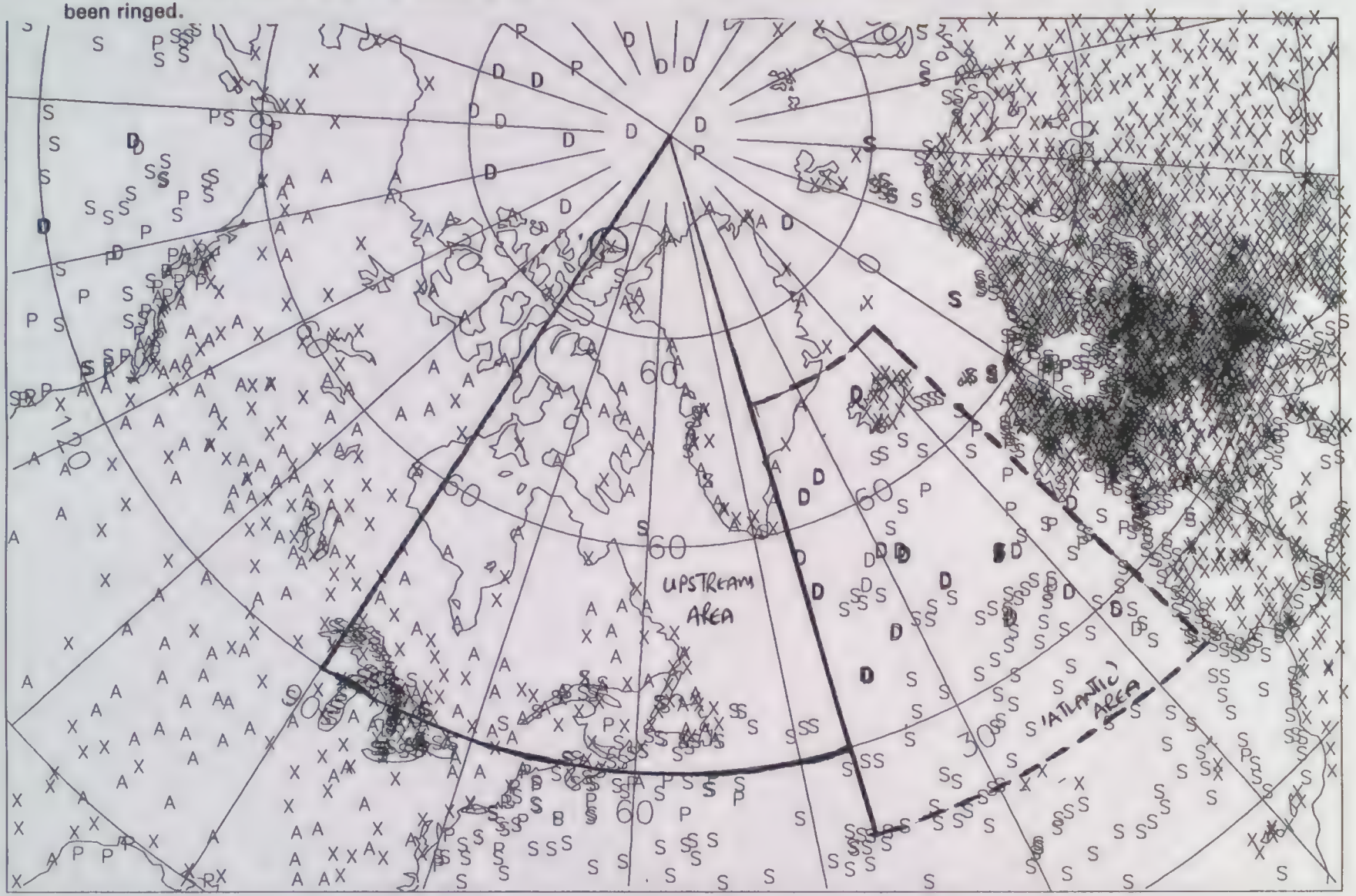

8350 OBS 7425 PLOTTED

4326 X SYNOP 1412 A ASYNOP 790 S SHIP 430 P ASHIP 467 D DRIFTR

Fig.5.

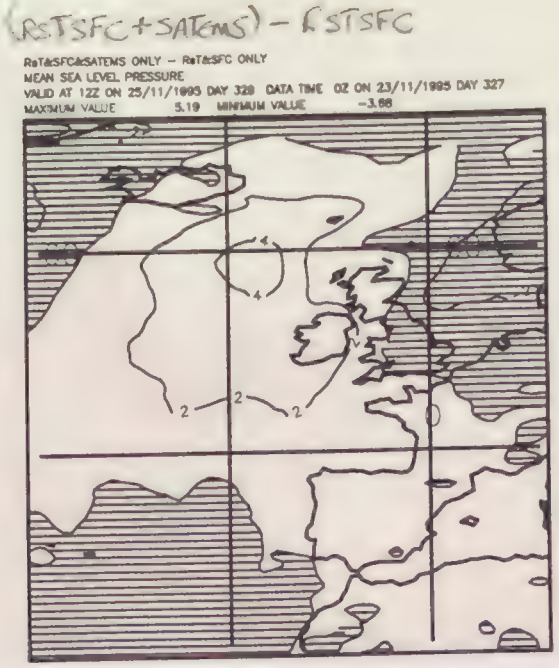

Fig.6) Difference between the RSTSFC plus NESDIS TOVS run and the RSTSFC run. Contouring conventions as in Fig.1d.

A1a) VERIFYING ANALYSIS T+ 0
POTENTIAL VORTICITY (300K) + THETA (850HPA)
VALID AT 12Z ON 25/11/1995 DAY 329 DATA TIME 12Z ON 25/11/1995 DAY 329
LEVEL: 300 K

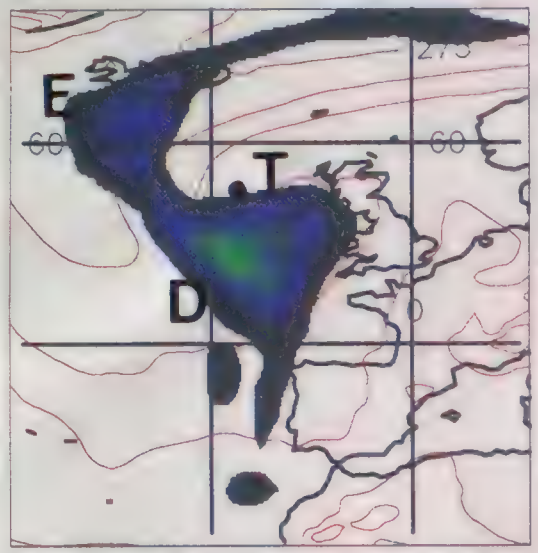

A1b) NO OBS T+60
POTENTIAL VORTICITY (300K) + THETA (850HPA)
VALID AT 12Z ON 25/11/1995 DAY 329 DATA TIME 12Z ON 22/11/1995 DAY 326
LEVEL: 300 K T+60

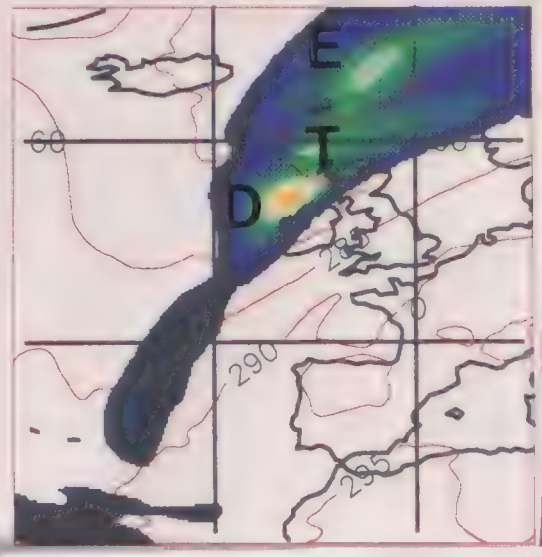

A1c) ALL OBS T+60
POTENTIAL VORTICITY (300K) + THETA (850HPA)
VALID AT 12Z ON 25/11/1995 DAY 329 DATA TIME OZ ON 23/11/1995 DAY 3
LEVEL: 300 K T+60

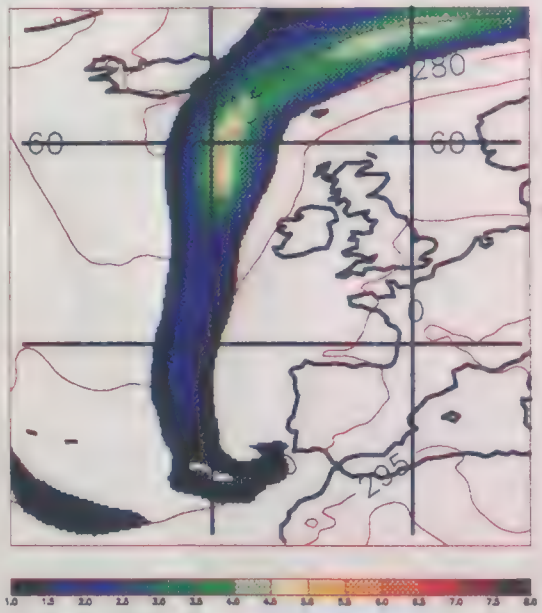

A1d) ALL OBS
POTENTIAL VORTICITY (300K) + THETA (850HPA)
VALID AT 12Z ON 25/11/1995 DAY 329 DATA
LEVEL: 300 K T+60

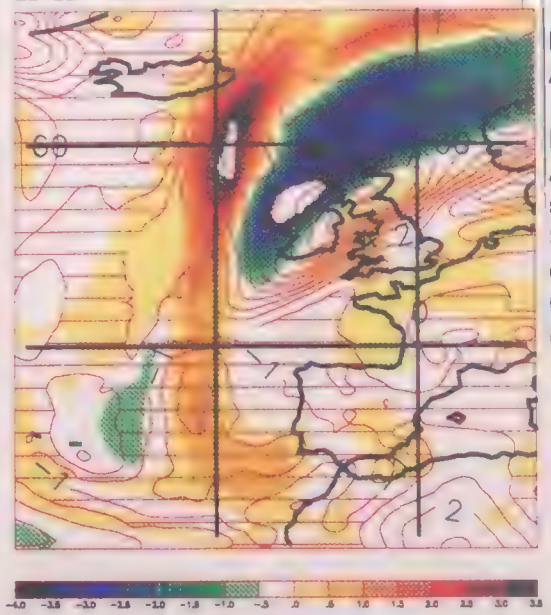

Fig.A1a)
Verifying analysis of PV(300K) (colour shading) and θ(850hPa) (contours) for 12GMT 25/11/95. Shading interval for PV = 0.5 unit, only values greater than 1 unit are shown. Contour interval for θ = 5K.

Fig.A1b)
NoOBS forecast of PV(300K) and θ(850hPa) valid at 12GMT 25/11/95. Plotting conventions as Fig.A1a.

Fig.A1c)
As Fig.A1b but for the AllOBS forecast.

Fig.A1d)
AllObs - NoOBS differences in forecast PV (colour shading) and θ (contours) valid 12GMT 25/11/95. Shading interval =0.5, red/yellow = positive differences; green/blue = negative differences. Contour interval = 1K (hatching indicates negative difference)

A2a) NO OBS T+ 0

POTENTIAL VORTICITY (300K) + THETA (850HPA)

VALID AT 0Z ON 23/11/1995 DAY 327 DATA TIME 12Z ON 22/11/1995 DAY 326

LEVEL: 300 K

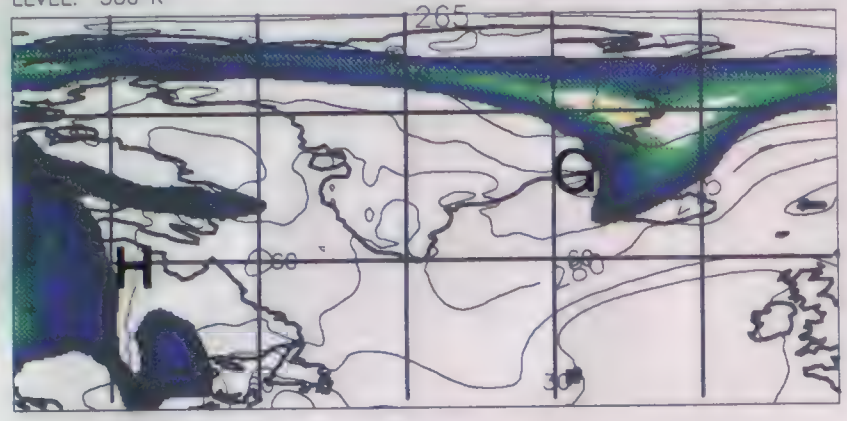

A2b) ALL OBS T+ 0

POTENTIAL VORTICITY (300K) + THETA (850HPA)

VALID AT 0Z ON 23/11/1995 DAY 327 DATA TIME 0Z ON 23/11/1995 DAY 327

LEVEL: 300 K

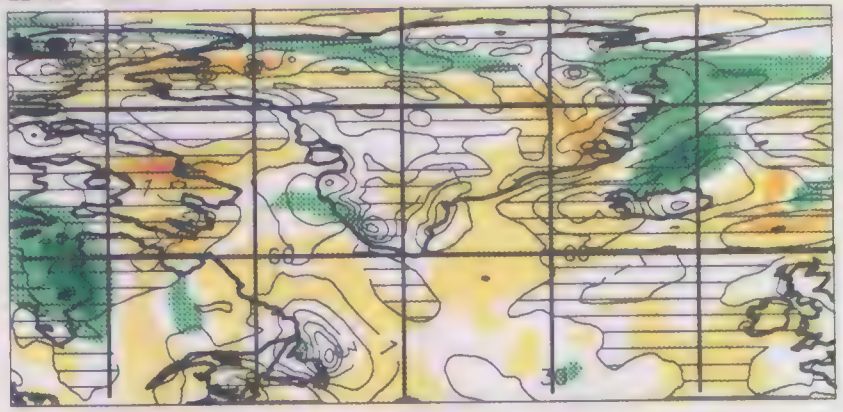

A2c) RsT Local RsTD T+ 0

POTENTIAL VORTICITY (300K) + THETA (850HPA)

VALID AT 0Z ON 23/11/1995 DAY 327 DATA TIME 0Z ON 23/11/1995 DAY 327

LEVEL: 300 K

A2d) RsT Upstream RsTU T+ 0

POTENTIAL VORTICITY (300K) + THETA (850HPA)

VALID AT 0Z ON 23/11/1995 DAY 327 DATA TIME 0Z ON 23/11/1995 DAY 327

LEVEL: 300 K

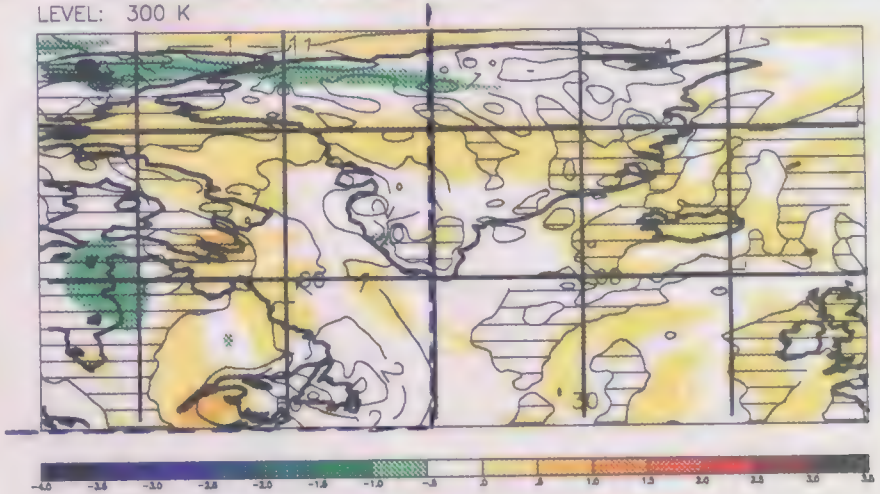

Fig.A2a) NoOBS PV(300K) and θ(850hPa) field at T+0. Plotting conventions as Fig.A1a.

Fig.A2b) AllOBS - NoOBS differences T+0. Plotting conventions as Fig.A1d.

Fig.A2c) As Fig.A2b, but for the RsTD run.

Fig.A2d) As Fig.A2b, but for the RsTU run.

A3a) NO OBS
POTENTIAL VORTICITY (300K) + THETA (850HPA)
VALID AT 0Z ON 24/11/1995 DAY 328 DATA TIME 12Z ON 22/11/1995 DAY 326
LEVEL: 300 K T+24

A3b) ALL OBS T+24
POTENTIAL VORTICITY (300K) + THETA (850HPA)
VALID AT 0Z ON 24/11/1995 DAY 328 DATA TIME 0Z ON 23/11/1995 DAY 327
LEVEL: 300 K T+24

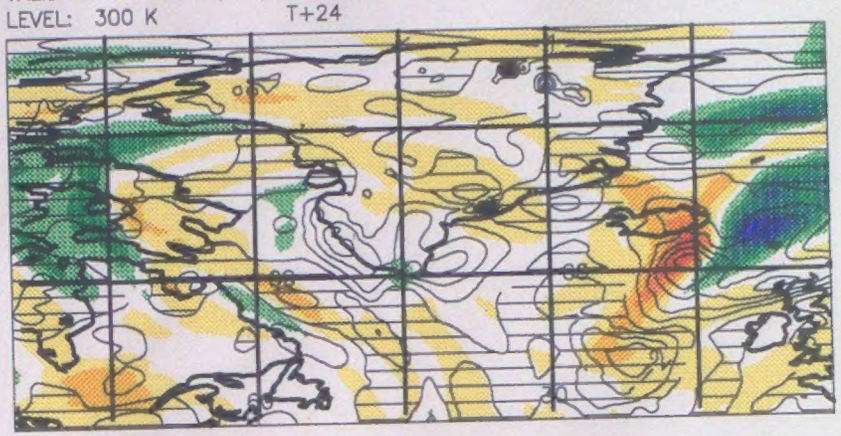

A3c) RsT Local RsTD T+24
POTENTIAL VORTICITY (300K) + THETA (850HPA)
VALID AT 0Z ON 24/11/1995 DAY 328 DATA TIME 0Z ON 23/11/1995 DAY 327
LEVEL: 300 K T+24

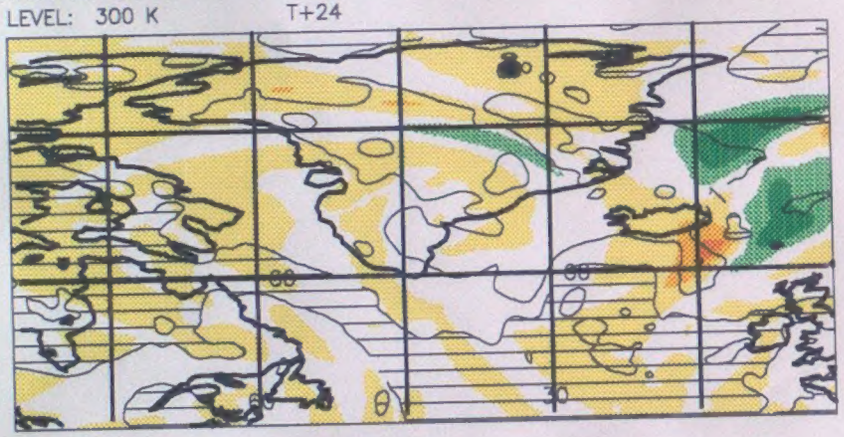

A3d) RsT Upstream RsTU T+24
POTENTIAL VORTICITY (300K) + THETA (850HPA)
VALID AT 0Z ON 24/11/1995 DAY 328 DATA TIME 0Z ON 23/11/1995 DAY 327
LEVEL: 300 K T+24

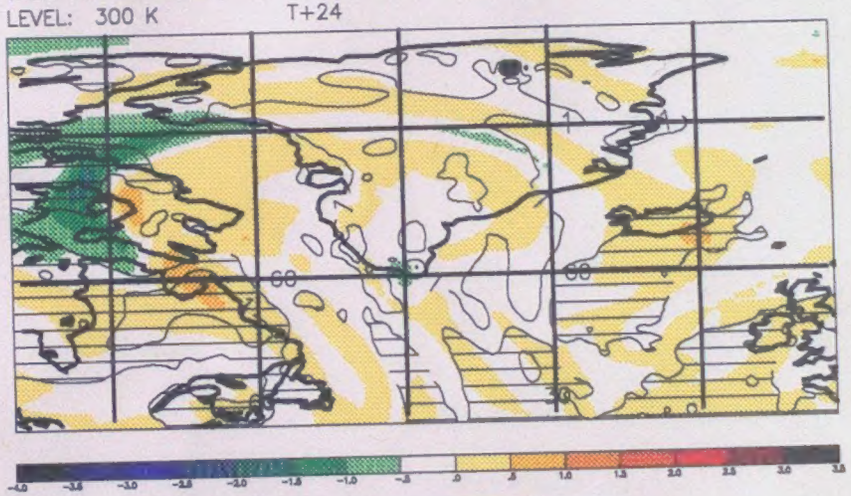

Fig.A3a) As Fig.A2a, but for T+24
Fig.A3b) As Fig.A2b, but for T+24
Fig.A3c) As Fig.A2c, but for T+24.
Fig.A3d) As Fig.A2d, but for T+24

A4a) NO OBS T+60
POTENTIAL VORTICITY (300K) + THETA (850HPA)
VALID AT 12Z ON 25/11/1995 DAY 329 DATA TIME 12Z ON 22/11/1995 DAY 326
LEVEL: 300 K T+60

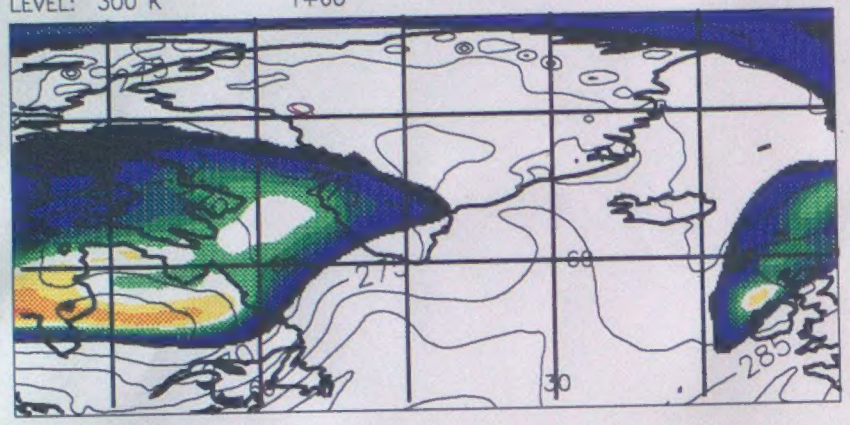

A4b) ALL OBS T+60
POTENTIAL VORTICITY (300K) + THETA (850HPA)
VALID AT 12Z ON 25/11/1995 DAY 329 DATA TIME 0Z ON 23/11/1995 DAY 327
LEVEL: 300 K T+60

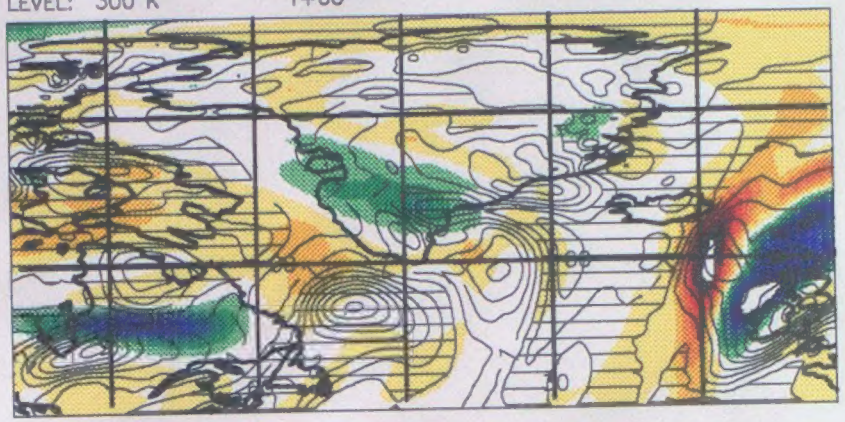

A4c) RsT Local RsTD T+60
POTENTIAL VORTICITY (300K) + THETA (850HPA)
VALID AT 12Z ON 25/11/1995 DAY 329 DATA TIME 0Z ON 23/11/1995 DAY 327
LEVEL: 300 K T+60

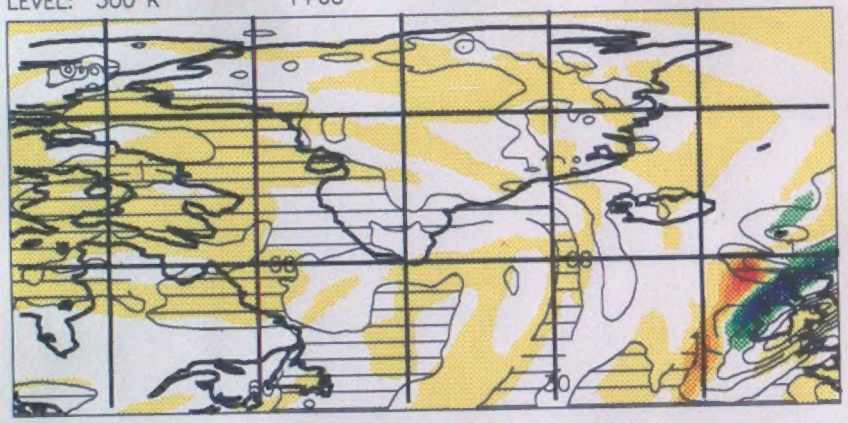

A4d) RsT Upstream RsTU T+60
POTENTIAL VORTICITY (300K) + THETA (850HPA)
VALID AT 12Z ON 25/11/1995 DAY 329 DATA TIME 0Z ON 23/11/1995 DAY 327
LEVEL: 300 K T+60

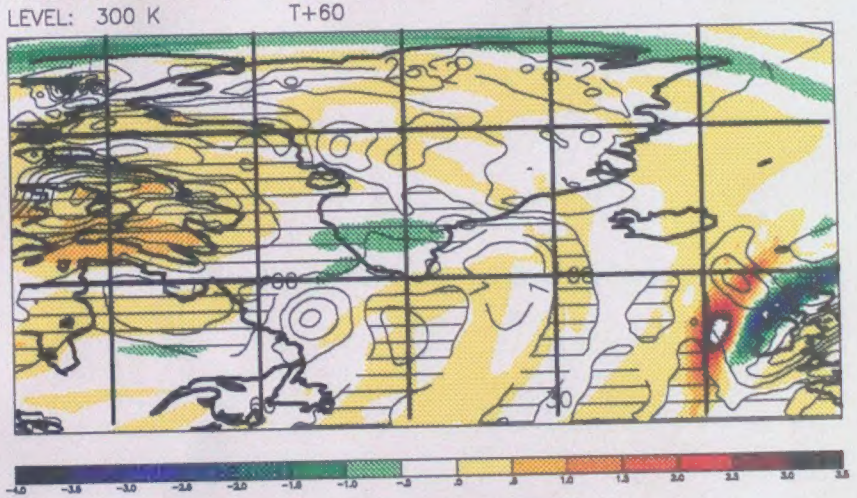

Fig.A4a) As Fig.A2a, but for T+60
Fig.A4b) As Fig.A2b, but for T+60
Fig.A4c) As Fig.A2c, but for T+60.
Fig.A4d) As Fig.A2d, but for T+60

A5a) NO OBS T+24
POTENTIAL VORTICITY (300K) + THETA (850HPA)
VALID AT 0Z ON 24/11/1995 DAY 328 DATA TIME 12Z ON 22/11/1995 DAY 326
LEVEL: 300 K T+24

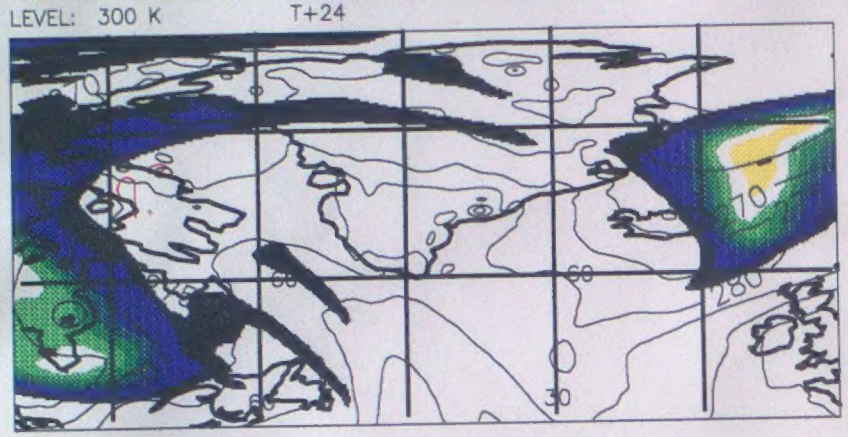

A5b) ALL OBS T+24
POTENTIAL VORTICITY (300K) + THETA (850HPA)
VALID AT 0Z ON 24/11/1995 DAY 328 DATA TIME 0Z ON 23/11/1995 DAY 327
LEVEL: 300 K T+24

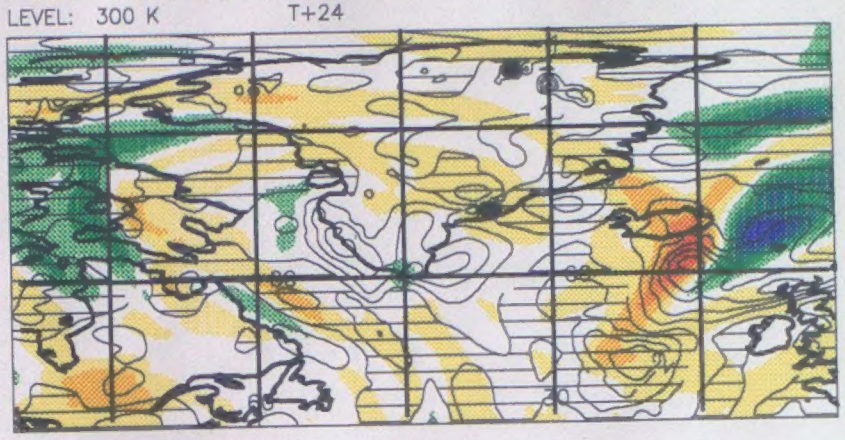

A5c) RsT (Local + Upstream) + Surface (Local) RSFCA T+24
POTENTIAL VORTICITY (300K) + THETA (850HPA)
VALID AT 0Z ON 24/11/1995 DAY 328 DATA TIME 0Z ON 23/11/1995 DAY 327
LEVEL: 300 K T+24

A5d) RsT (Local + Upstream) + Surface (Upstream) RSFCU T+24
POTENTIAL VORTICITY (300K) + THETA (850HPA)
VALID AT 0Z ON 24/11/1995 DAY 328 DATA TIME 0Z ON 23/11/1995 DAY 327
LEVEL: 300 K T+24

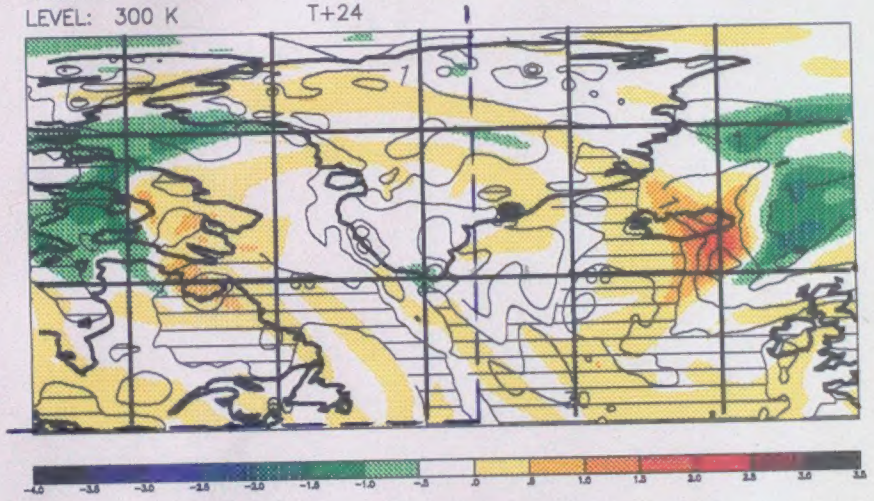

Fig.A5a)	Same as Fig.A3a.	Fig.A5c)	As Fig.A3c, but for the RSFCA run.
Fig.A5b)	Same as Fig.A3b	Fig.A5d)	As Fig.A3d, but for the RSFCU run.

A6a) NO OBS T+60
POTENTIAL VORTICITY (300K) + THETA (850HPA)
VALID AT 12Z ON 25/11/1995 DAY 329 DATA TIME 12Z ON 22/11/1995 DAY 326
LEVEL: 300 K T+60

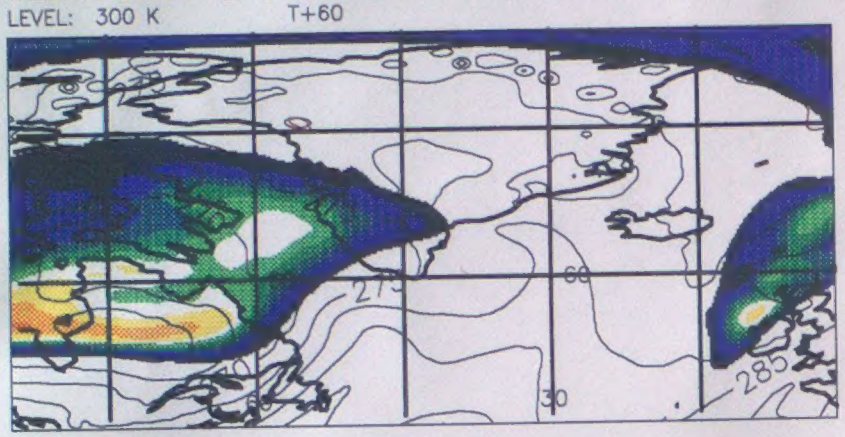

A6b) ALL OBS T+60
POTENTIAL VORTICITY (300K) + THETA (850HPA)
VALID AT 12Z ON 25/11/1995 DAY 329 DATA TIME 0Z ON 23/11/1995 DAY 327
LEVEL: 300 K T+60

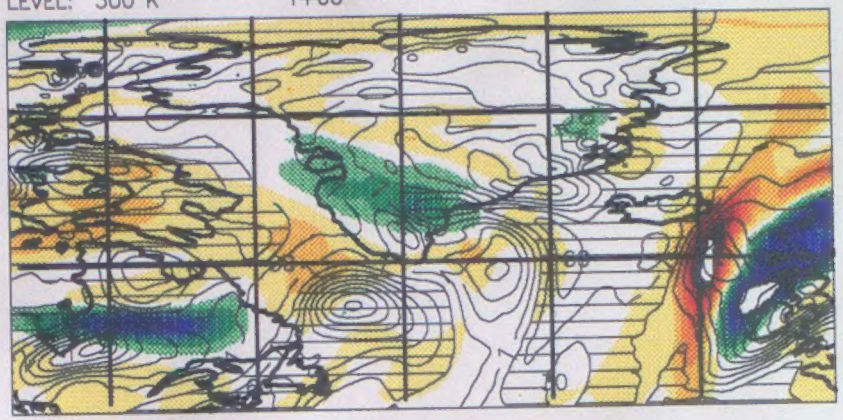

A6c) RsT (Local + Upstream) + Surface (Local) RSFCA T+60
POTENTIAL VORTICITY (300K) + THETA (850HPA)
VALID AT 12Z ON 25/11/1995 DAY 329 DATA TIME 0Z ON 23/11/1995 DAY 327
LEVEL: 300 K T+60

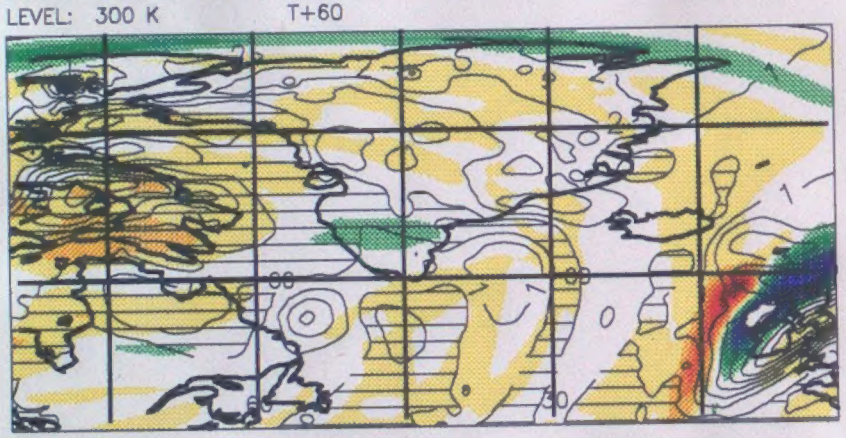

A6d) RsT (Local + Upstream) + Surface (Upstream) RSFCU T+60
POTENTIAL VORTICITY (300K) + THETA (850HPA)
VALID AT 12Z ON 25/11/1995 DAY 329 DATA TIME 0Z ON 23/11/1995 DAY 327
LEVEL: 300 K T+60

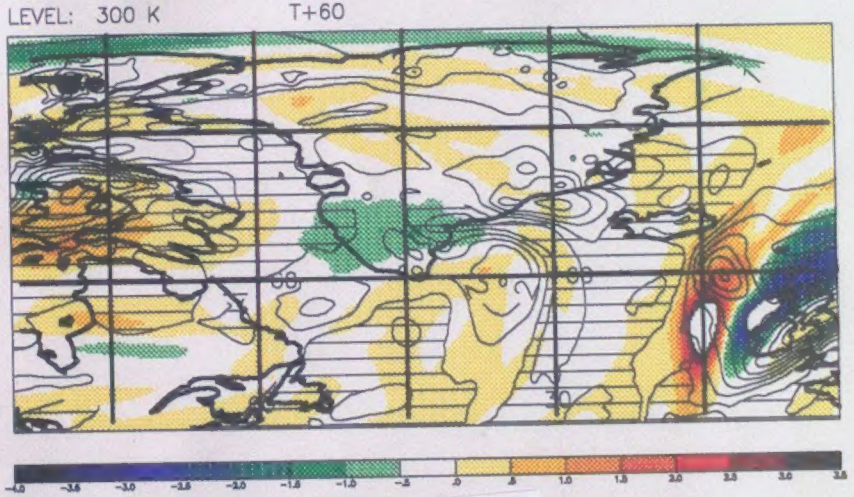

Fig.A6a) Same as Fig.A4a.
Fig.A6b) Same as Fig.A4b
Fig.6c) As Fig.A5c, but for T+60
Fig.6d) As Fig.A5d, but for T+60